

## **Supplementary Information**

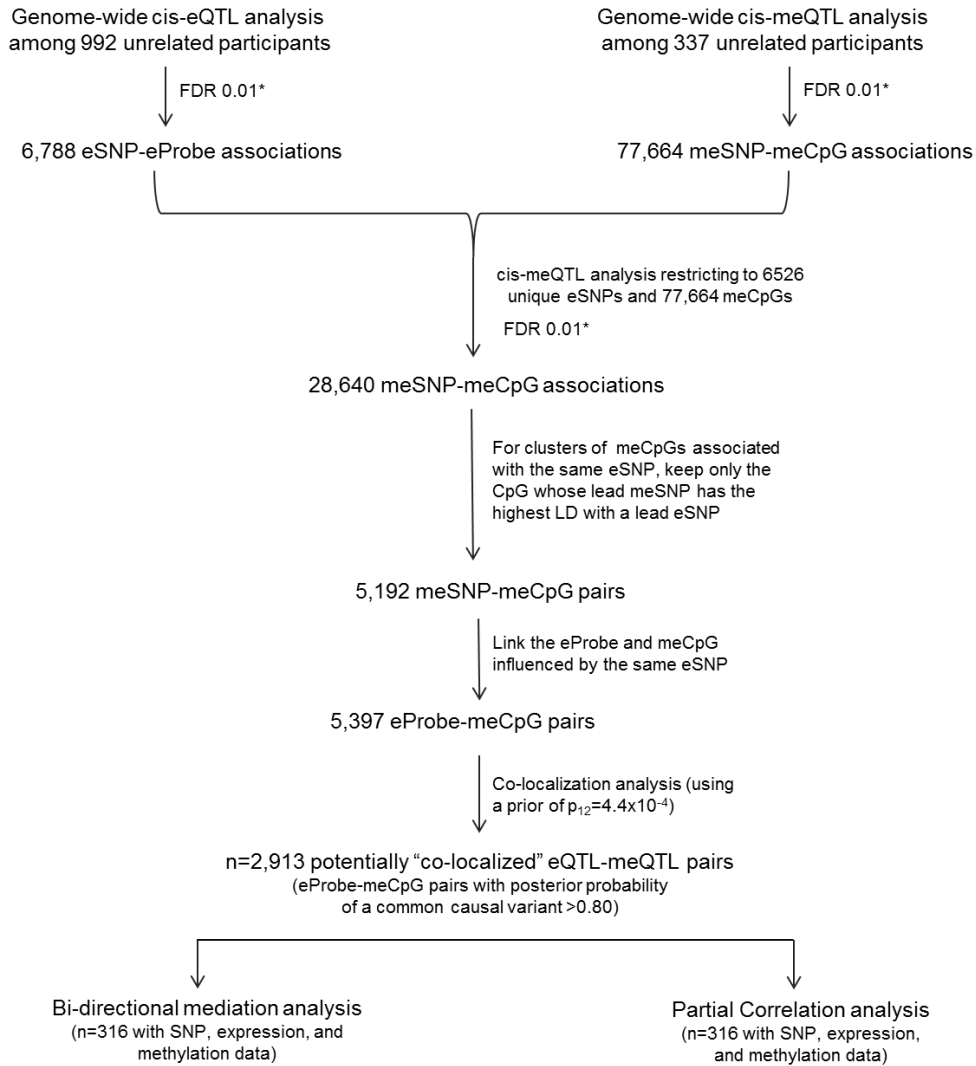
**Co-occurring expression and methylation QTLs allow detection of common causal variants and shared biological mechanisms**

**Pierce, et al.**

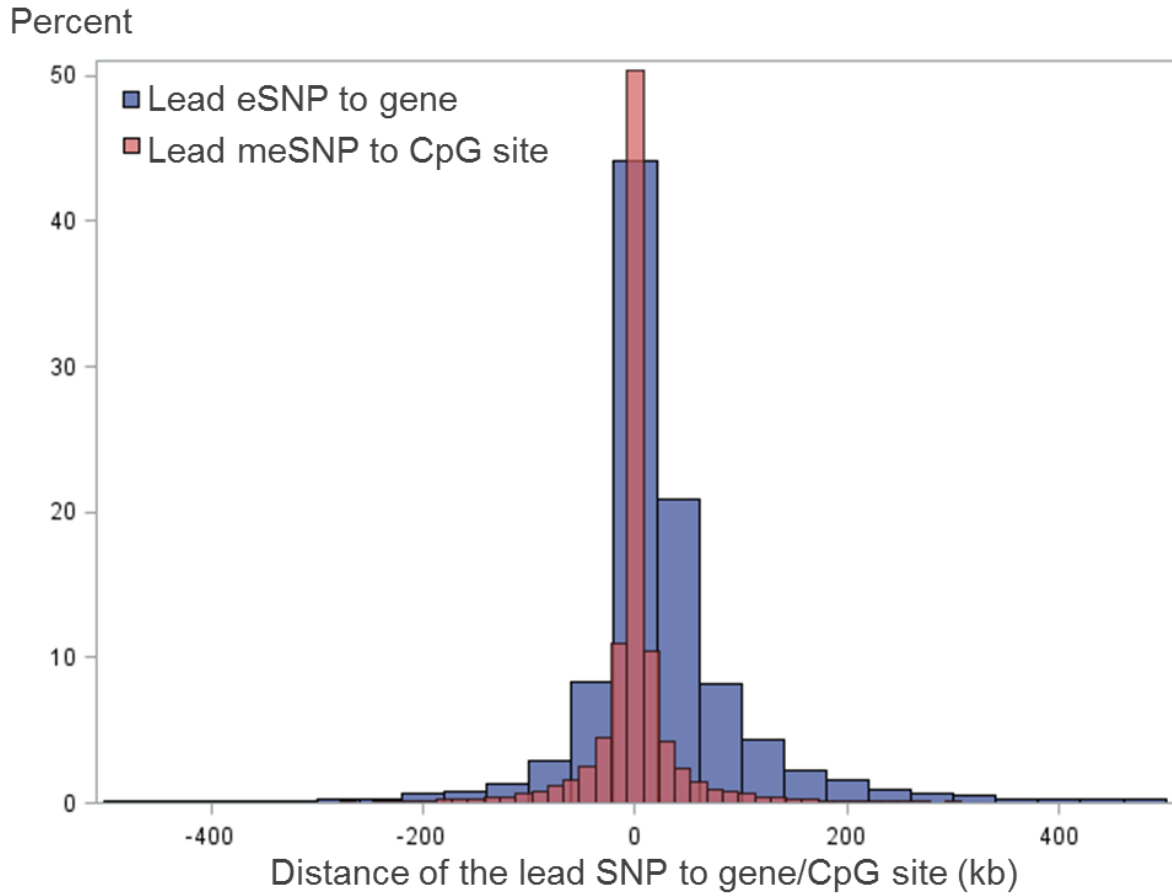
**Supplementary Table 1. Logistic regression of Sobel P (SME) <0.05, Sobel P (SEM) <0.05, and Partial correlation P<0.05 on eQTL/meQTL P-values**

Predictors	Outcome					
	Sobel P (SME) <0.05		Sobel P (SEM) <0.05		Corr. P<0.05	
	OR (95%CI)	p-value	OR (95%CI)	p-value	OR (95%CI)	p-value
<b>cis-eQTL P-value quartiles</b>						
Quartile 1 (largest P-value)	1	Ref	1	Ref	1	Ref
Quartile 2	1.63 (1.10, 2.42)	0.02	3.38 (1.84, 6.22)	<.0001	1.32 (0.95, 1.82)	0.1
Quartile 3	2.61 (1.80, 3.77)	<.0001	7.56 (4.27, 13.40)	<.0001	1.86 (1.36, 2.53)	<.0001
Quartile 4 (smallest P-value)	2.91 (2.02, 4.19)	<.0001	9.86 (5.61, 17.33)	<.0001	2.21 (1.64, 3.00)	<.0001
<b>cis-meQTL P-value quartiles</b>						
Quartile 1 (largest P-value)	1	Ref	1	Ref	1	Ref
Quartile 2	1.41 (0.95, 2.08)	0.09	1.38 (0.90, 2.11)	0.14	1.15 (0.84, 1.58)	0.39
Quartile 3	2.02 (1.40, 2.92)	0.0002	1.99 (1.33, 2.96)	0.0008	1.45 (1.07, 1.97)	0.02
Quartile 4 (smallest P-value)	3.04 (2.14, 4.31)	<.0001	2.65 (1.80, 3.90)	<.0001	2.06 (1.54, 2.77)	<.0001

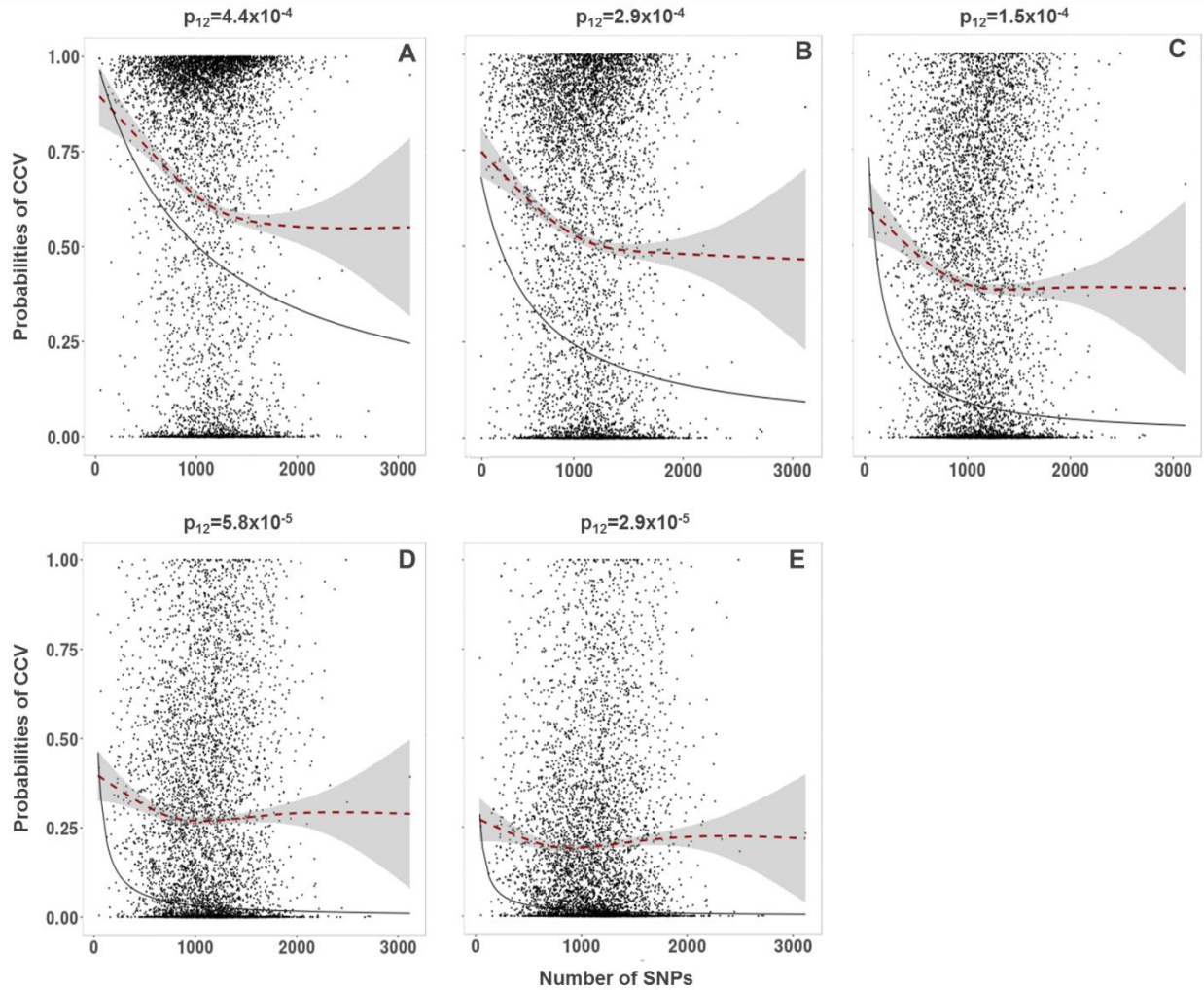
The sample size consists of 2,913 gene expression probe-SNP-CpG trios with posterior probability of one common causal variant >0.80.



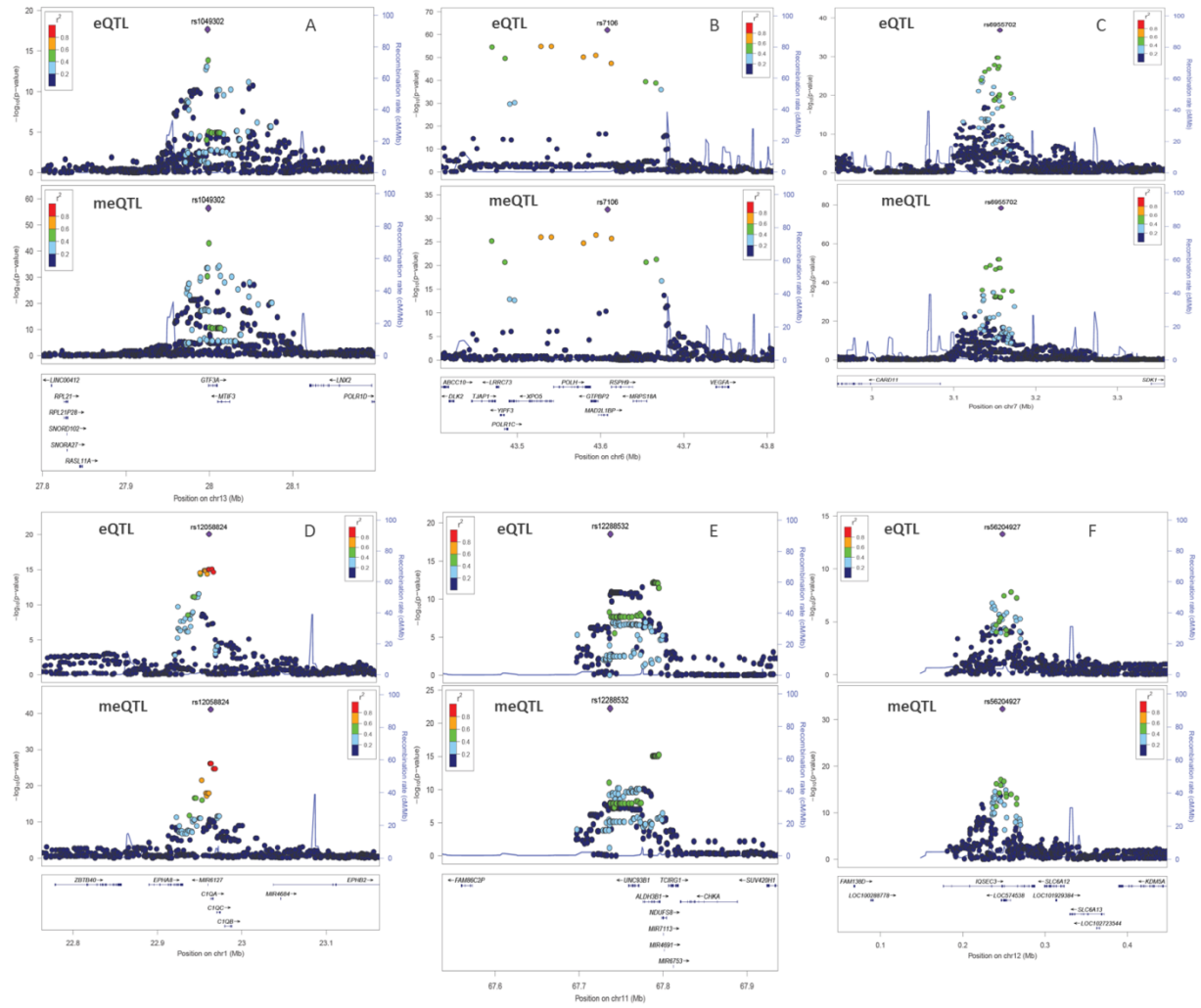
**Supplementary Figure 1. Workflow for identifying eQTLs, meQTLs, and co-localized eQTL-meQTL pairs.** \*Beta distribution-adjusted empirical p-values from FastQTL were used to calculate q-values (Storey & Tibshirani, PNAS, 2003), and a false discovery rate (FDR) threshold of <0.01 was applied at the probe level to identify eProbes/meCpGs with a significant eQTL/meQTL.



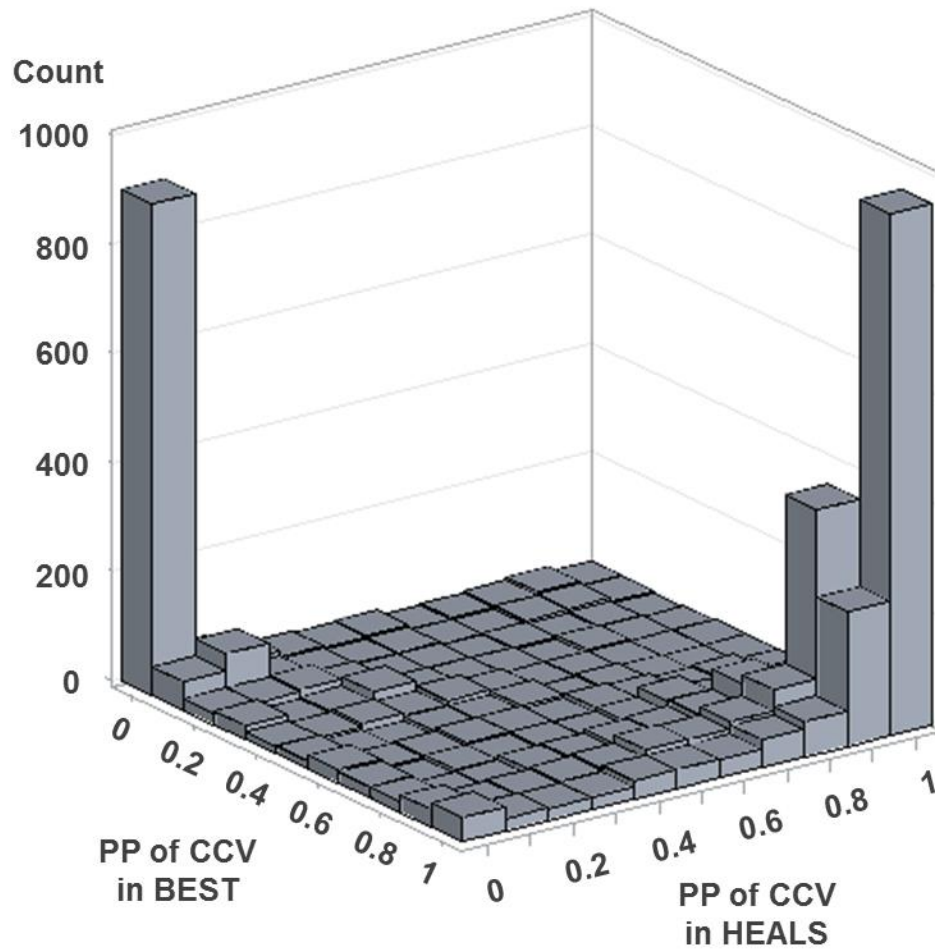
**Supplementary Figure 2. Distance of the lead eSNP to the transcript start site of the target gene (n=6,788) and the distance of the lead meSNP to the affected CpG site (n=77,664).**



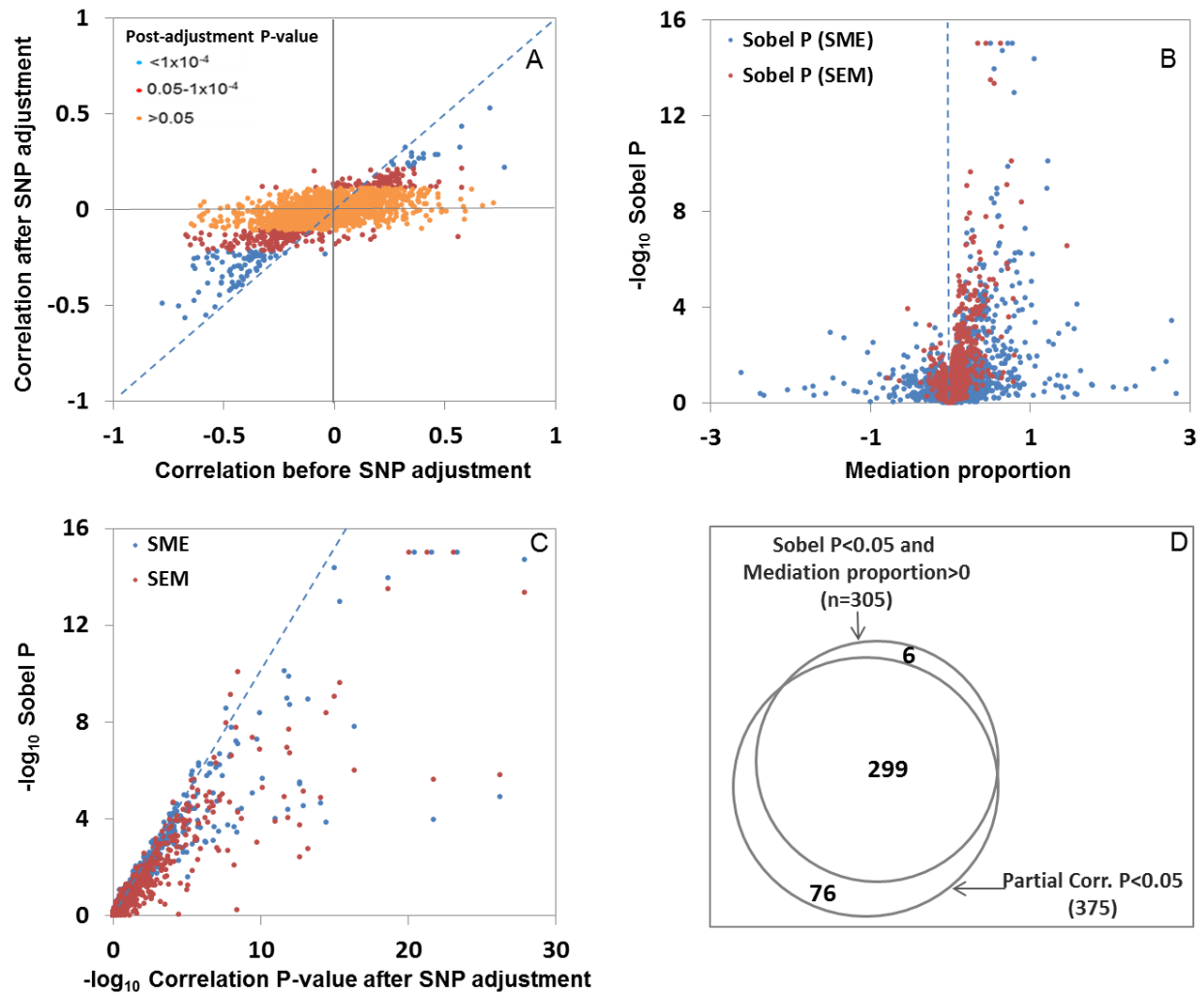
**Supplementary Figure 3. Effect of choice of prior probability ( $p_{12}$ ) of common causal variant (CCV) on the posterior probability of a CCV.** For each eQTL-meQTL pair undergoing co-localization analyses, we plotted the relative posterior support for a CCV (as opposed to distinct causal variants, DCV) for each co-localization test, defined by  $PP \text{ of CCV} / (PP \text{ of DCV} + PP \text{ of CCV})$ , against the number of SNPs used for each co-localization test. The red dotted line is the Loess smoothing curve of these points. The black solid line is the relative prior support for a CCV, based on the values selected the priors ( $p_1$ ,  $p_2$ , and  $p_{12}$ ), calculated using the equation provided by Guo *et al.*<sup>22</sup> This data is restricted to co-localization tests with a posterior probability of two distinct causal variants ( $PP \text{ of DCV}$ ) + posterior probability of common causal variant ( $PP \text{ of CCV}$ ) > 0.8 (100 out of 5397 tests excluded).



**Supplementary Figure 4. Locus zoom plots for 6 examples of co-localized eQTL-meQTL pairs in Figure 3.** The color of the dots in the eQTL plots reflects the LD  $r^2$  level to the lead meSNP for the corresponding CpG site and the color of the dots in the meQTL plots reflects the LD  $r^2$  level to the lead eSNP for the corresponding gene.

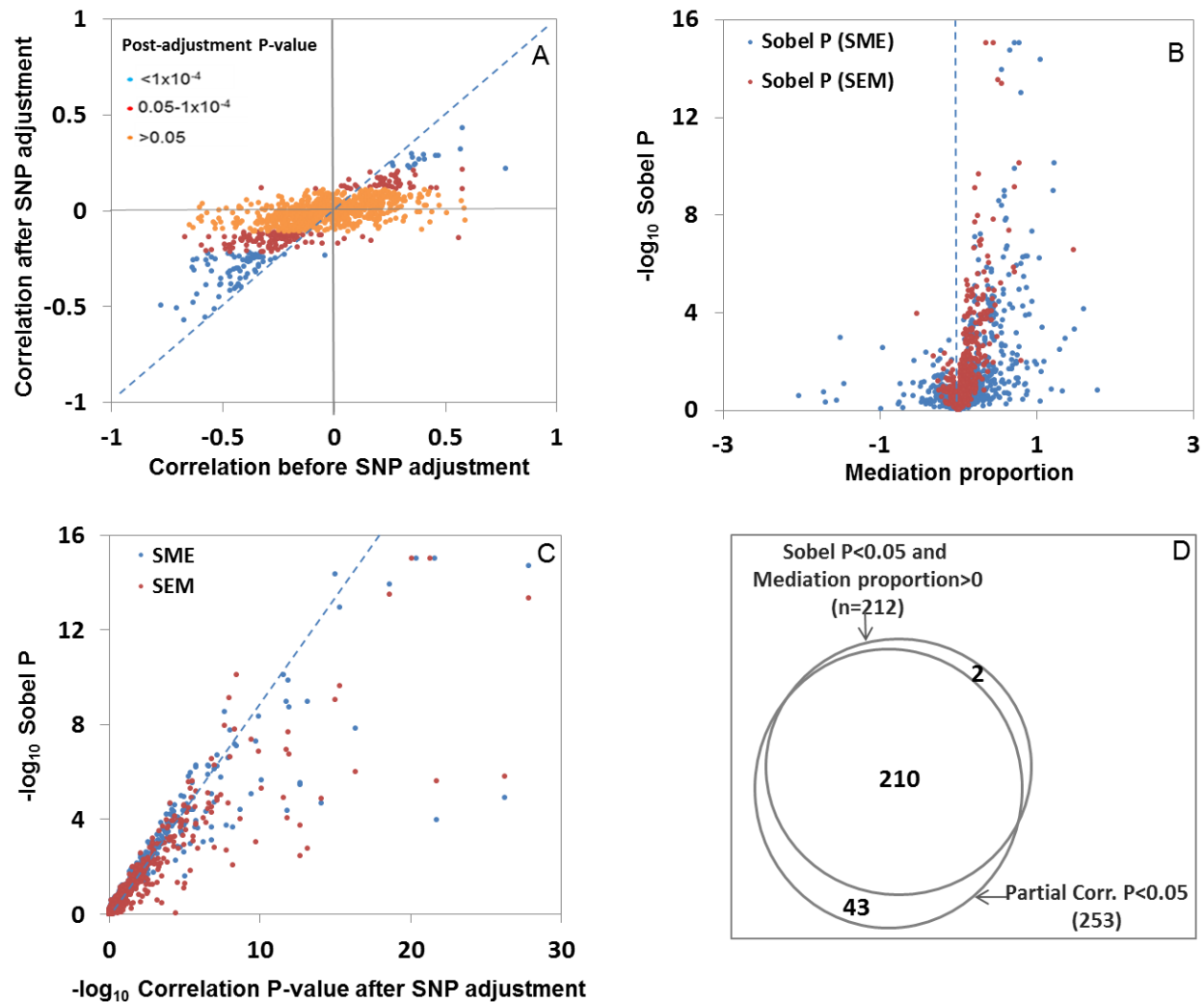


**Supplementary Figure 5. Results of replication of co-localization analyses for 4,875 eQTL-meQTL pairs.** The histogram compares the posterior probability (PP) of a common causal variant (CCV) based on BEST methylation data (450K array) to PP of CCV based on HEALS methylation data (EPIC array). Both analyses use a  $p_{12}$  value of  $4.4 \times 10^{-4}$ .

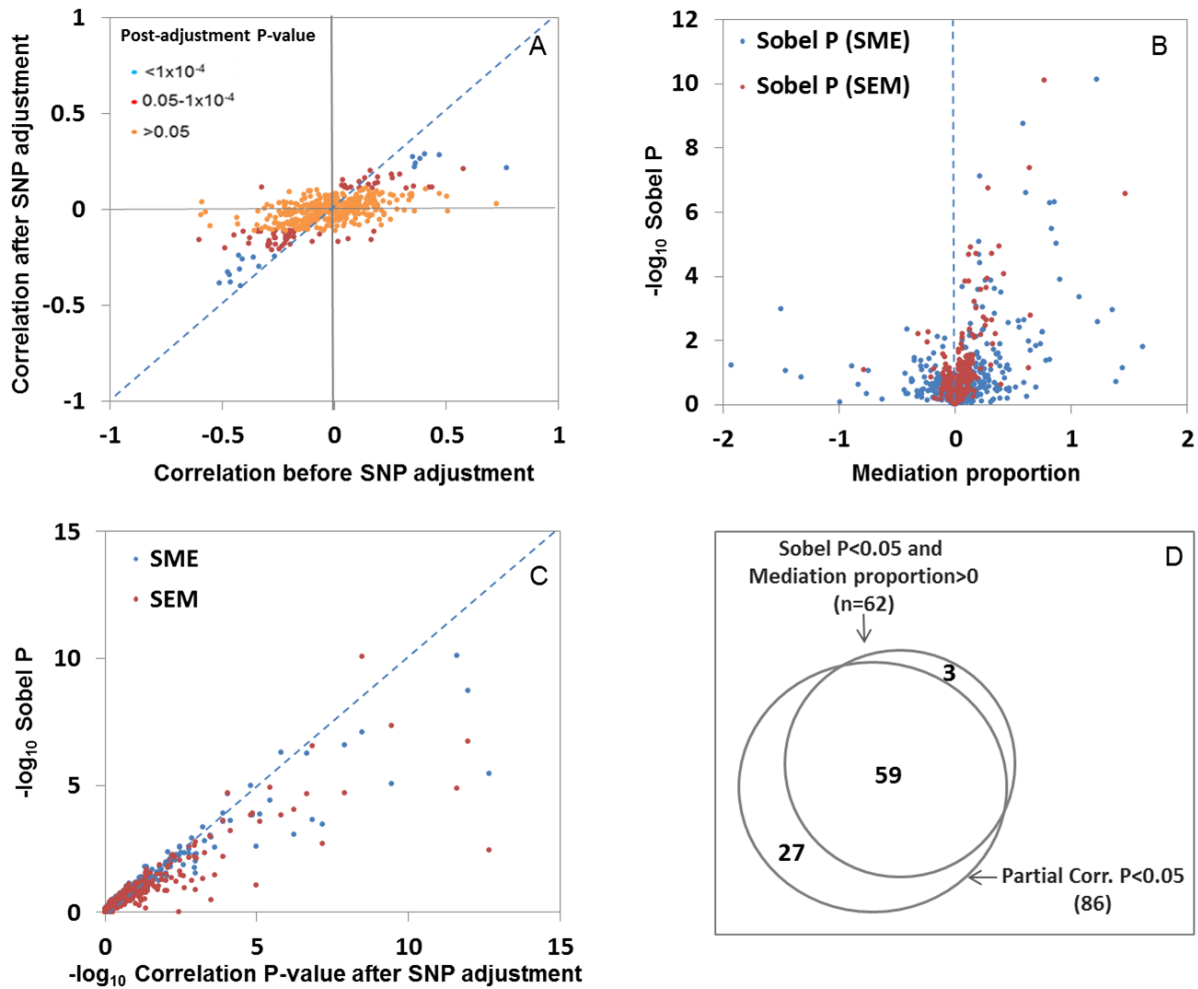


**Supplementary Figure 6. Partial correlation and mediation analyses provide evidence for shared a regulatory mechanism ( $p_{12}=2.9 \times 10^{-4}$ ).** Model for each of 2,098 potentially co-localized eQTL-mQTL pairs (using  $p_{12}=2.9 \times 10^{-4}$ ) includes adjustments for age, sex, and PCs from both the expression and methylation data (n=316). A: results from partial correlation analysis. B: Mediation analysis results for the SME and the SEM model. Mediation proportion outliers out of -3 to 3 ranges were removed from the figure and Sobel P outliers  $< 10^{-15}$  were set to the  $10^{-15}$ . C: Relationship between Sobel P from mediation analyses and the post-adjustment correlation P values from partial correlation analysis. Sobel P outliers  $< 10^{-15}$  were set to the  $10^{-15}$ . D: Venn diagram showing the concordance between mediation analysis and partial correlation analyses.

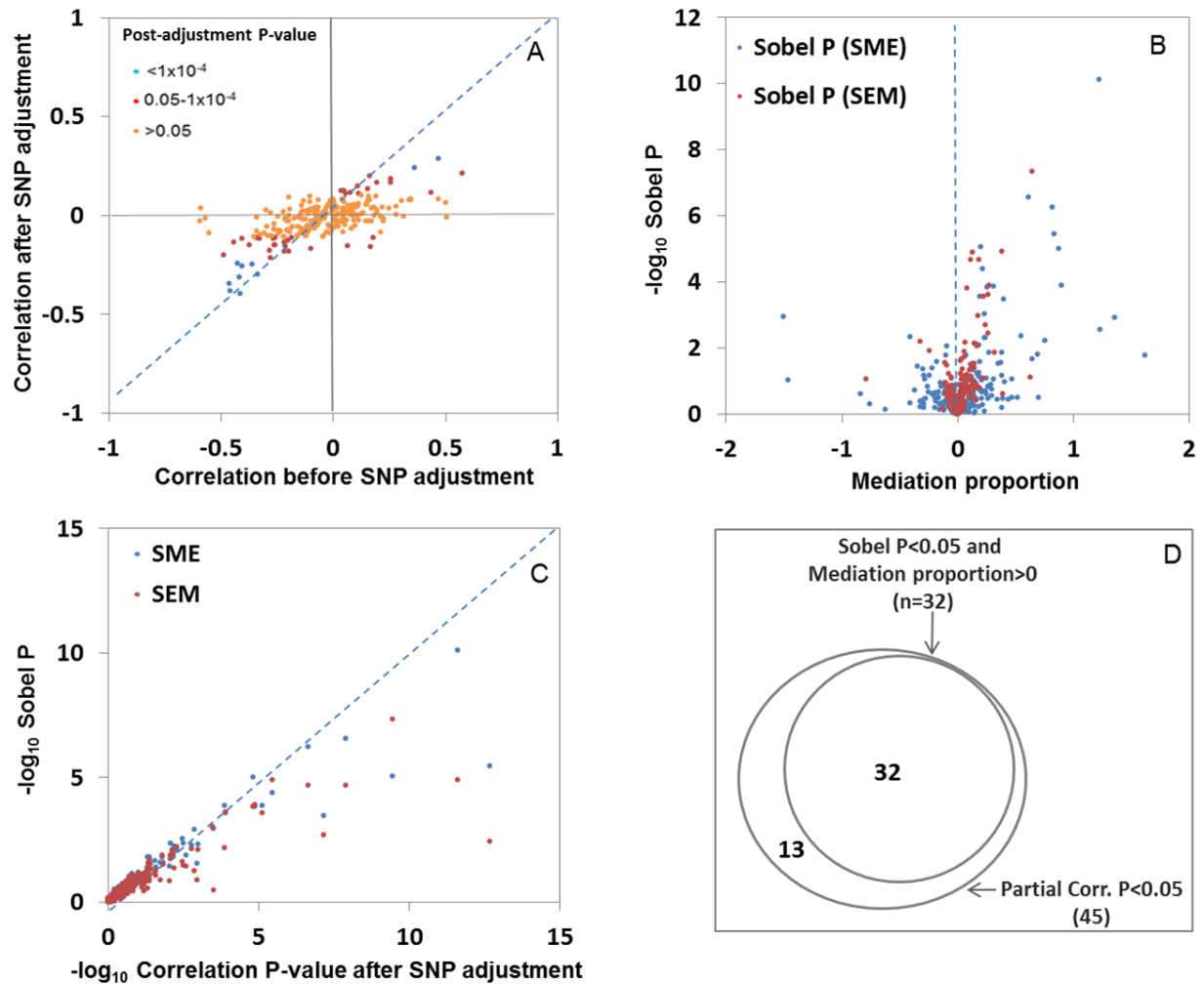




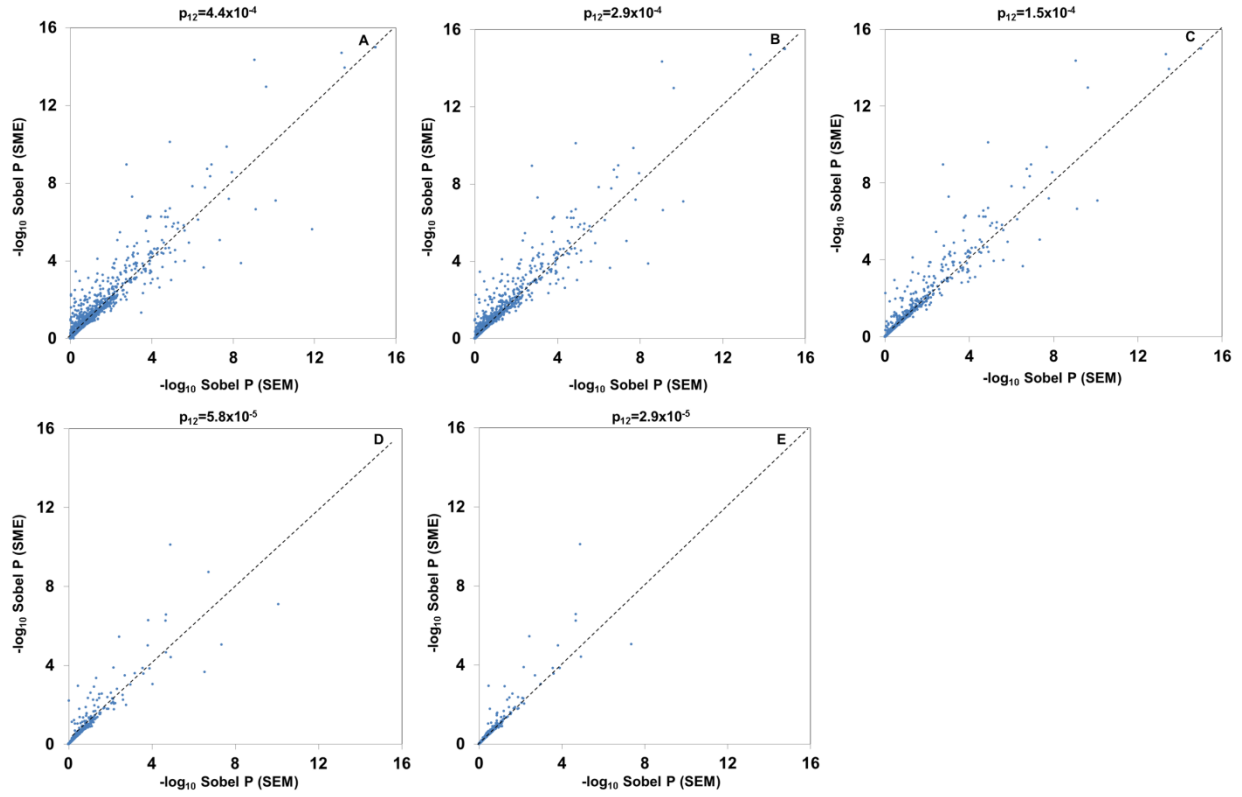
**Supplementary Figure 7. Partial correlation and mediation analyses provide evidence for shared a regulatory mechanism ( $p_{12}=1.45 \times 10^{-4}$ ).** Model for each of 1,047 potentially co-localized eQTL-mQTL pairs (using  $p_{12}=1.45 \times 10^{-4}$ ) includes adjustments for age, sex, and PCs from both the expression and methylation data ( $n=316$ ). A: results from partial correlation analysis. B: Mediation analysis results for the SME and the SEM model. Mediation proportion outliers out of -3 to 3 ranges were removed from the figure and Sobel P outliers  $<10^{-15}$  were set to the  $10^{-15}$ . C: Relationship between Sobel P from mediation analyses and the post-adjustment correlation P values from partial correlation analysis. Sobel P outliers  $<10^{-15}$  were set to the  $10^{-15}$ . D: Venn diagram showing the concordance between mediation analysis and partial correlation analyses.



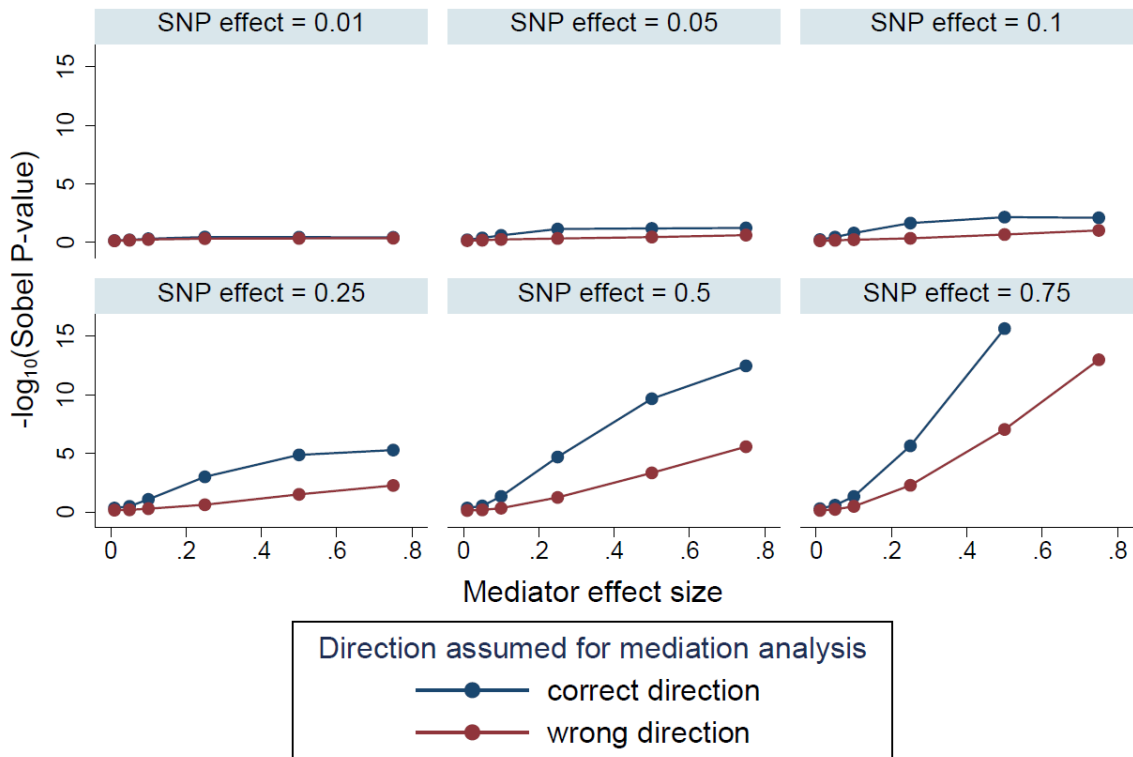
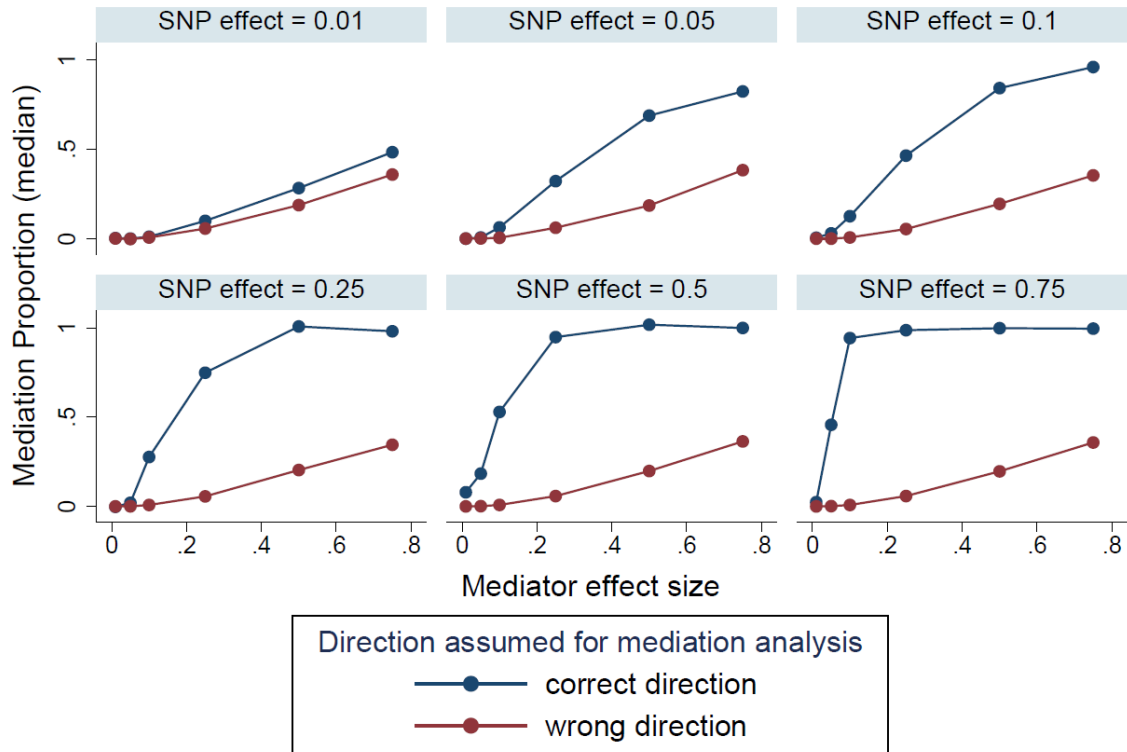
**Supplementary Figure 8. Partial correlation and mediation analyses provide evidence for shared a regulatory mechanism ( $p_{12} = 5.8 \times 10^{-5}$ ).** Model for each of 473 potentially co-localized eQTL-mQTL pairs includes adjustments for age, sex, and PCs from both the expression and methylation data ( $n = 316$ ). A: results from partial correlation analysis. B: Mediation analysis results for the SME and the SEM model. C: Relationship between Sobel P from mediation analyses and the post-adjustment correlation P values from partial correlation analysis. D: Venn diagram showing the concordance between mediation analysis and partial correlation analyses.



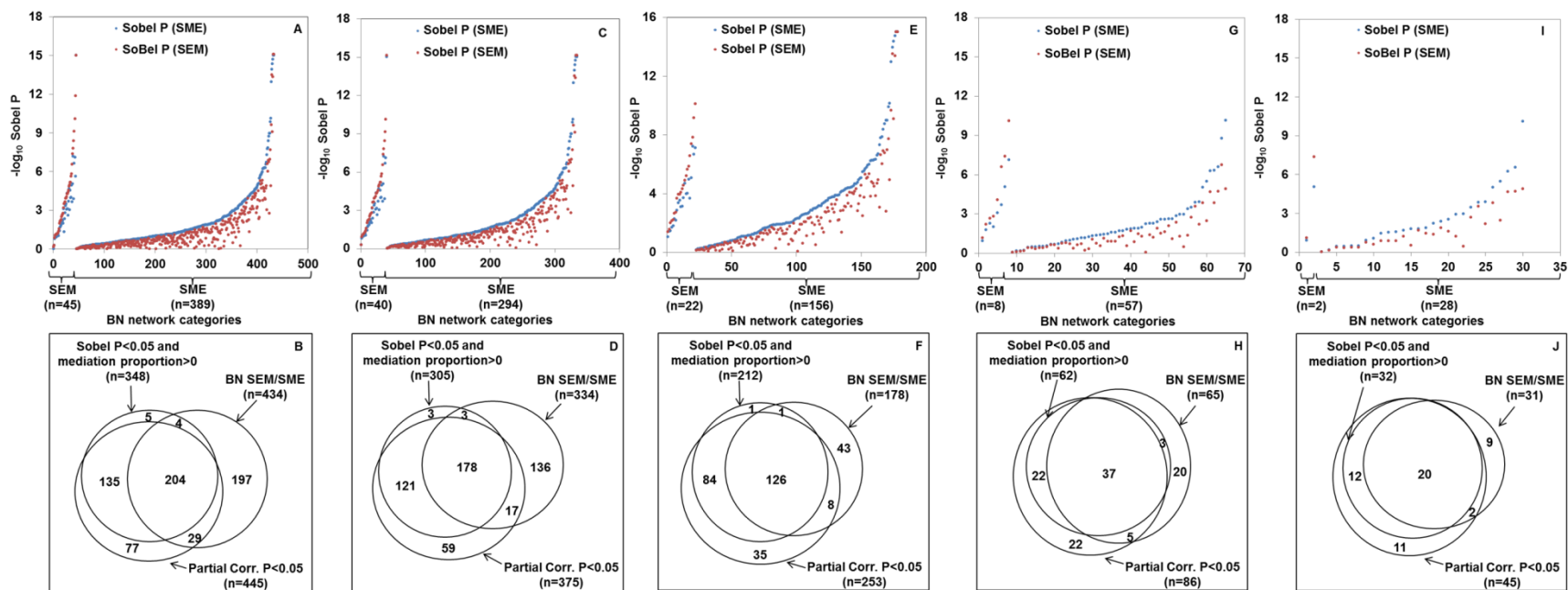
**Supplementary Figure 9. Partial correlation and mediation analyses provide evidence for shared a regulatory mechanism ( $p_{12}=2.9 \times 10^{-5}$ ).** Model for each of 266 potentially co-localized eQTL-mQTL pairs includes adjustments for age, sex, and PCs from both the expression and methylation data ( $n=316$ ). A: results from partial correlation analysis. B: Mediation analysis results for the SME and the SEM model. C: Relationship between Sobel P from mediation analyses and the post-adjustment correlation P values from partial correlation analysis. D: Venn diagram showing the concordance between mediation analysis and partial correlation analyses.



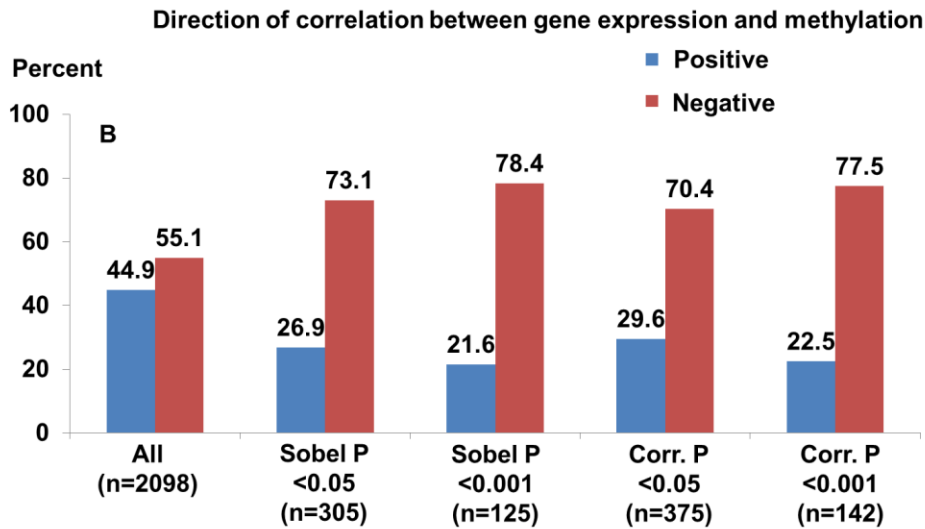
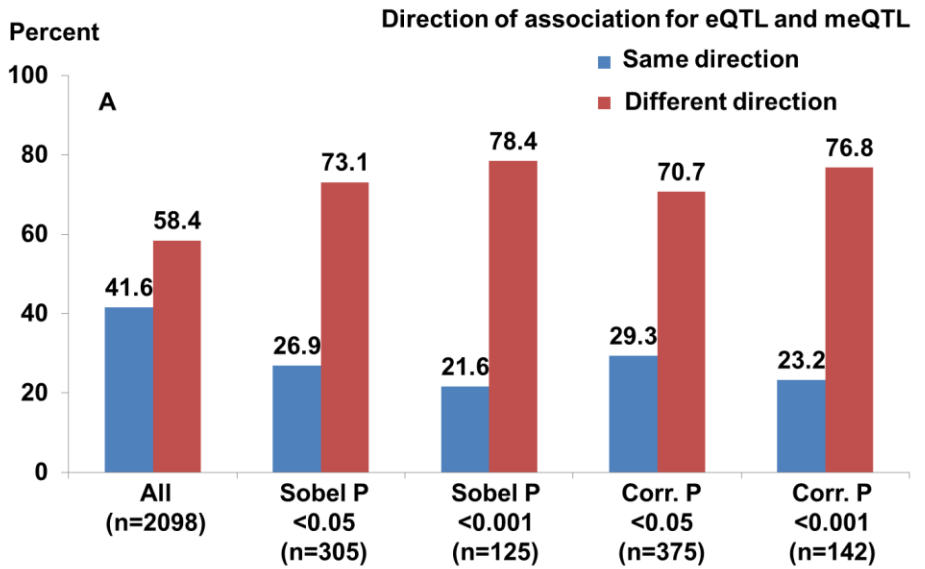
**Supplementary Figure 10. Scatter plots of Sobel P values for SME and SEM models.** A:  $p_{12}=4.4 \times 10^{-4}$ ; B:  $p_{12}=2.9 \times 10^{-4}$ , C:  $p_{12}=1.45 \times 10^{-4}$ , D:  $p_{12}=2.8 \times 10^{-5}$ , E:  $p_{12}=2.9 \times 10^{-5}$



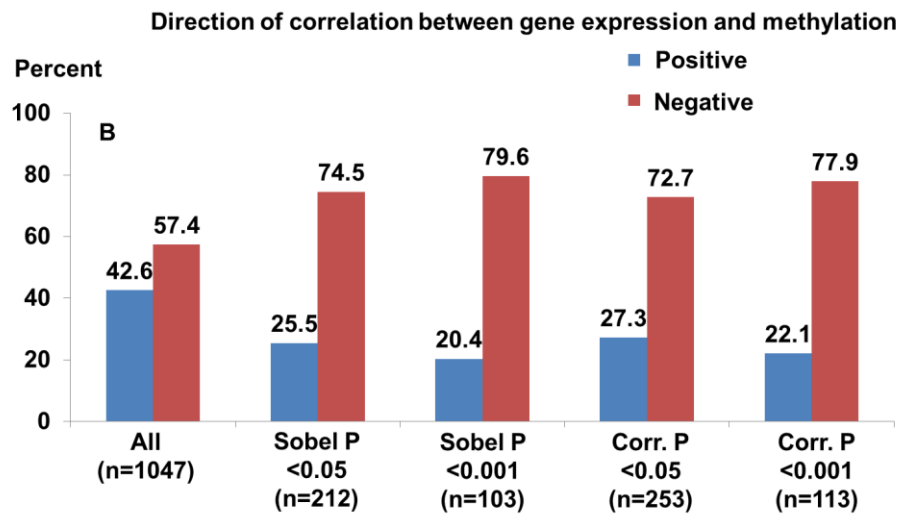
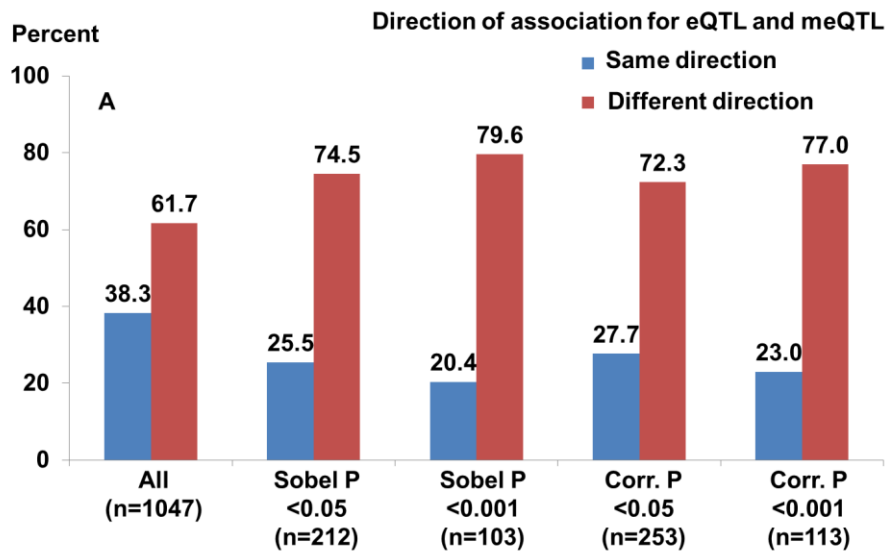
**Supplementary Figure 11. Evidence for mediation will be stronger when the correct model is specified.** Results are based on simulated data of sample size 316. The top panel reports the mediation proportion and the bottom panel reports the  $-\log_{10}(\text{Sobel P})$ , varying the effect sizes of the SNP and the mediator.



**Supplementary Figure 12. Results from mediation analysis compared with Bayesian Network and partial correlation analyses.** Upper panel: Sobel P values plotted according to the causal model selected by Bayesian network analyses. Lower panel: Venn Diagram demonstrating concordance among three methods for assessing evidence for a shared regulatory mechanism. Plot A and B:  $p_{12}=4.4 \times 10^{-4}$ , Plot C and D:  $p_{12}=2.9 \times 10^{-4}$ , Plot E and F:  $p_{12}=1.5 \times 10^{-4}$ , Plot G and H:  $p_{12}=5.8 \times 10^{-5}$ , Plot I and J:  $p_{12}=2.9 \times 10^{-5}$ .

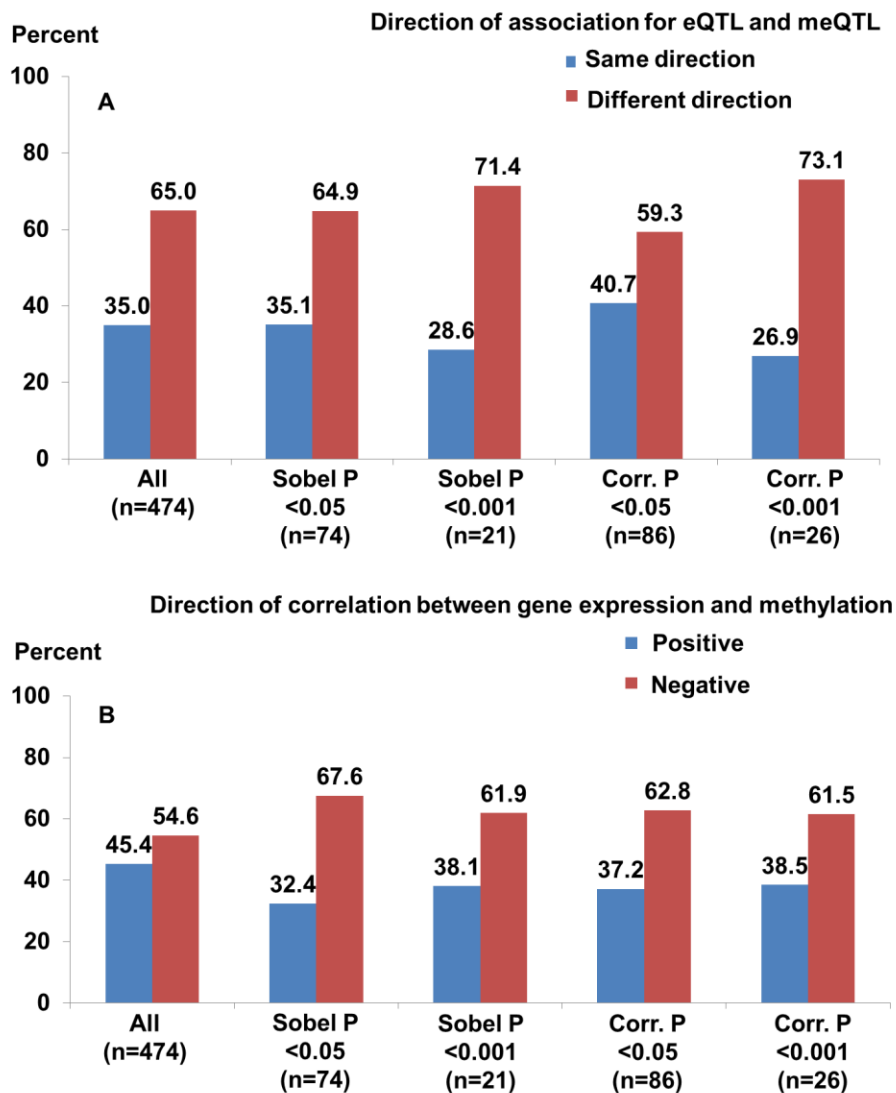


**Supplementary Figure 13. Direction of QTL effects and associations between expression and methylation for co-localized eQTL-meQTL pairs.** Co-localized pairs using a  $p_{12}$  value  $2.9 \times 10^{-4}$  are presented. Results are stratified according to P-values from mediation analysis (Sobel P) and partial correlation analysis (Corr. P). A: Histograms of the percentage of eQTL-meQTL pairs showing the same or different direction of association. B: Histograms of the percentage of eQTL-meQTL pairs for which the direction of association between gene expression and DNA methylation is positive or negative.

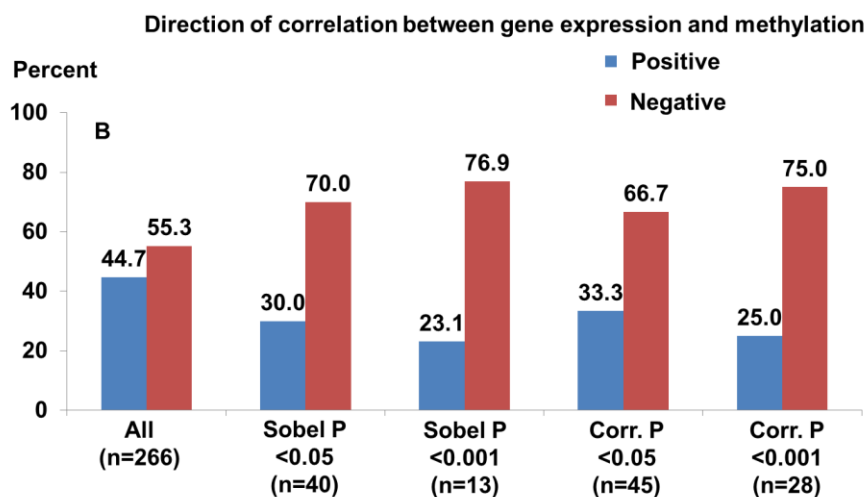
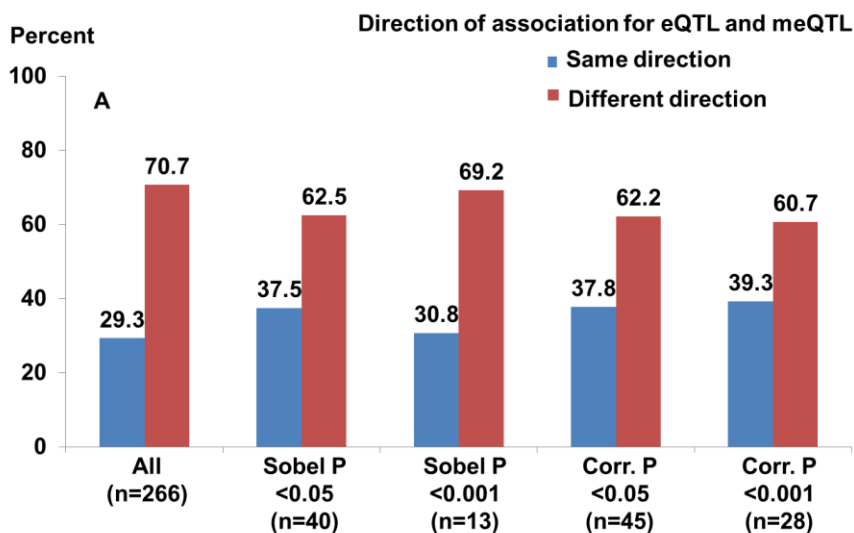


**Supplementary Figure 14. Direction of QTL effects and associations between expression and methylation for co-localized eQTL-meQTL pairs.** Co-localized pairs using a  $p_{12}$  value  $1.45 \times 10^{-4}$  are presented. Results are stratified according to P-values from mediation analysis (Sobel P) and partial correlation analysis (Corr. P). A: Histograms of the percentage of eQTL-meQTL pairs showing the same or different direction of association. B: Histograms of the percentage of eQTL-meQTL pairs for which the direction of association between gene expression and DNA methylation is positive or negative.

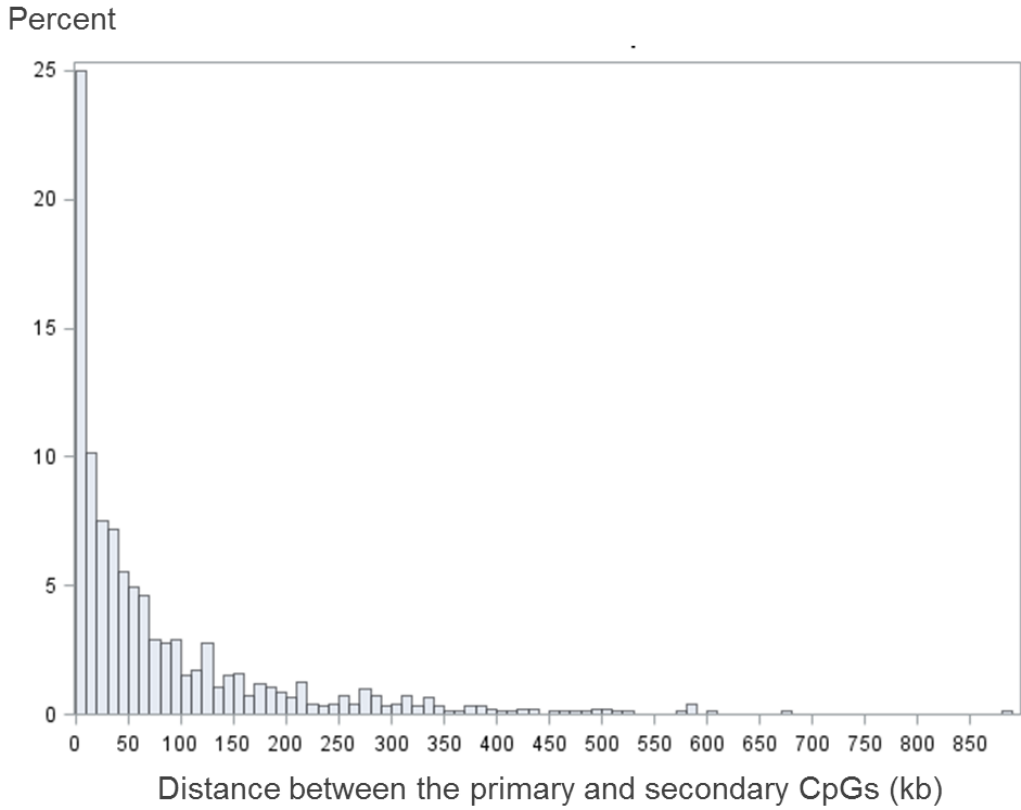




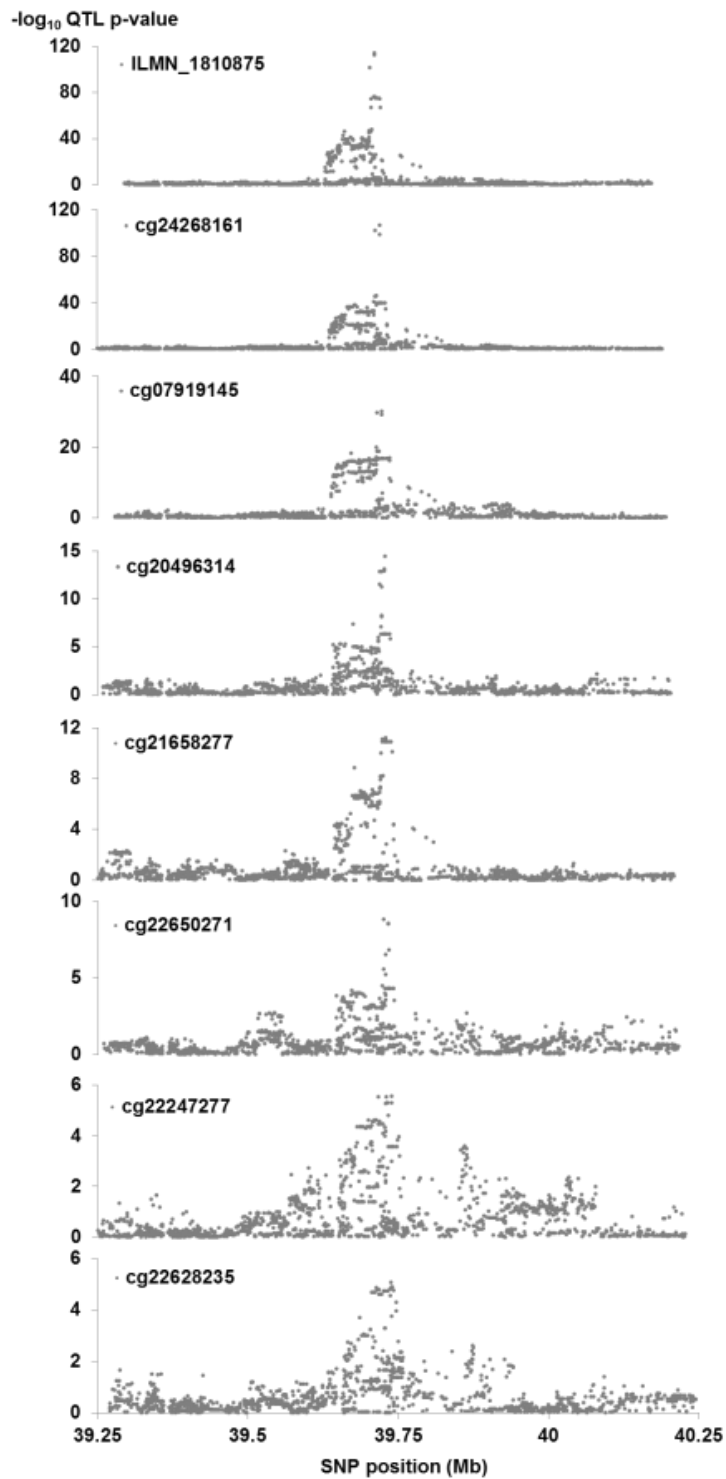
**Supplementary Figure 15. Direction of QTL effects and associations between expression and methylation for co-localized eQTL-meQTL pairs.** Co-localized pairs using a  $p_{12}$  value  $5.8 \times 10^{-5}$  are presented. Results are stratified according to P-values from mediation analysis (Sobel P) and partial correlation analysis (Corr. P). A: Histograms of the percentage of eQTL-meQTL pairs showing the same or different direction of association. B: Histograms of the percentage of eQTL-meQTL pairs for which the direction of association between gene expression and DNA methylation is positive or negative.



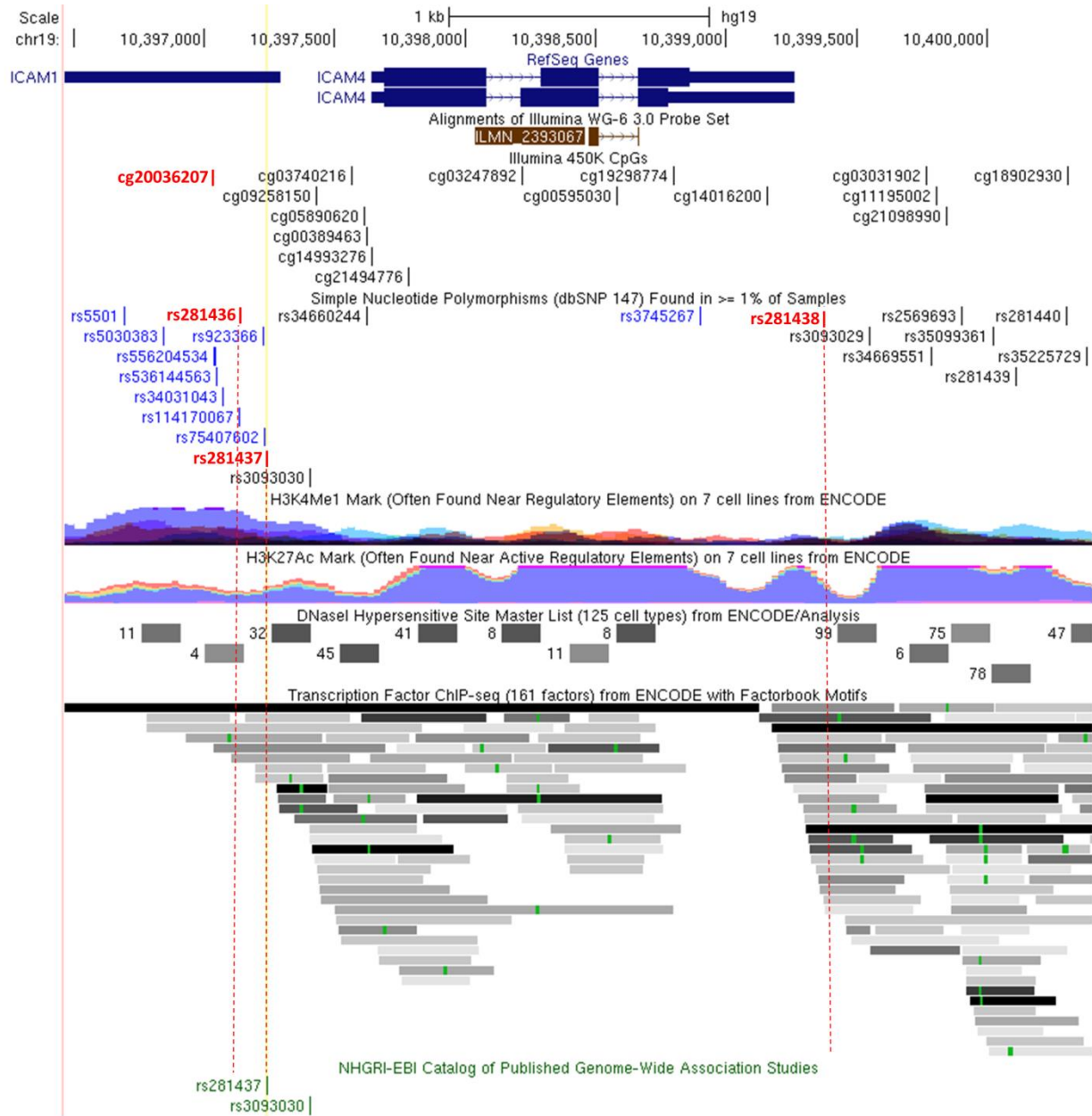
**Supplementary Figure 16. Direction of QTL effects and associations between expression and methylation for co-localized eQTL-meQTL pairs.** Co-localized pairs using a  $p_{12}$  value  $2.9 \times 10^{-5}$  are presented. Results are stratified according to P-values from mediation analysis (Sobel P) and partial correlation analysis (Corr. P). A: Histograms of the percentage of eQTL-meQTL pairs showing the same or different direction of association. B: Histograms of the percentage of eQTL-meQTL pairs for which the direction of association between gene expression and DNA methylation is positive or negative.



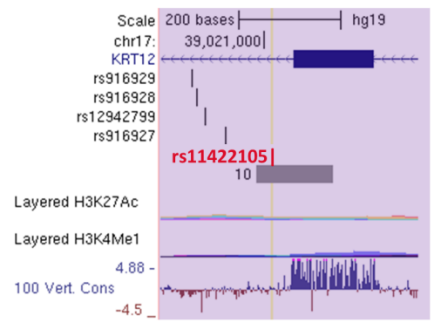
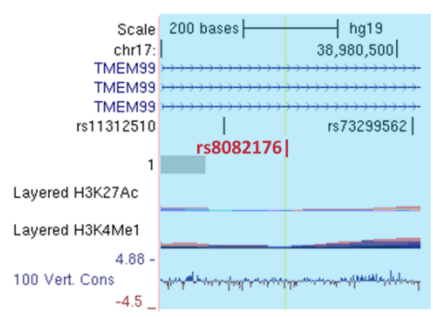
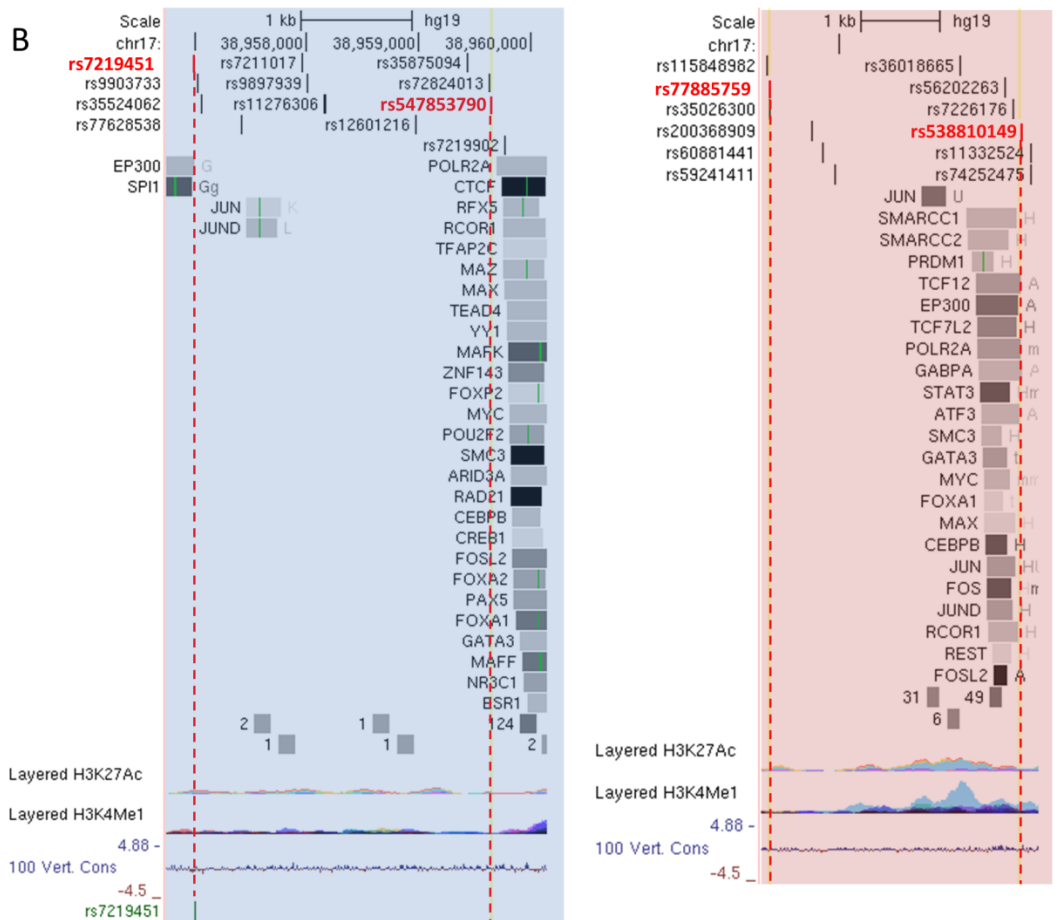
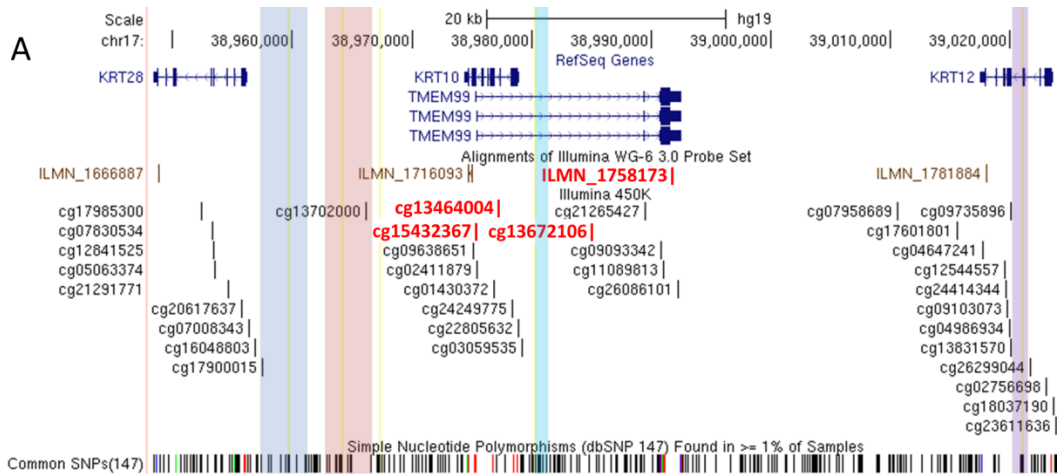
**Supplementary Figure 17.** Distribution of distance between the primary and secondary CpGs for n=955 cases with expression and primary methylation in the same direction but have at least one secondary CpG inversely associated with the CpG originally selected.



**Supplementary Figure 18. Regional association plots for one eQTL affecting *SYNGR1* (ILMN\_1810875) a co-localizing meQTL that affects seven nearby CpGs. The genomic region to which these association plots correspond is shown in Figure 8.**



**Supplementary Figure 19. Overlap with genomic annotations for three candidate causal SNPs for a co-localized eQTL-meQTL pair that shows strong evidence of mediation.** Expression of the ICAM4 gene and methylation at nearby CpG cg20036207 (in red) are affected by a common causal variant. SNP rs281437 was the lead *cis*-eSNP for ILMN\_2393067 ( $P=10^{-23}$ ) which captures expression of all RefSeq isoforms of ICAM4. This eQTL co-localizes with a meQTL affecting methylation at cg20036207 (Probability of CCV $>99\%$ ), with strong evidence of partial correlation (residual  $r = -0.30$ ,  $P=5 \times 10^{-8}$ ) and mediation (SEM  $P = 2 \times 10^{-5}$ ; SME  $P = 6 \times 10^{-7}$ ). This SNP is in strong LD ( $r^2 > 0.65$ ) with only two SNPs in the Bangladeshi population (1KG BEB), rs281436 ( $r^2 = 0.97$ ) and rs281438 ( $r^2 = 0.77$ ). The two SNPs showing the strongest association with methylation AND expression, rs281437 and rs281436, reside 107 bp apart, and rs281436 is  $\sim 100$  bp from cg20036207.



**Supplementary Figure 20. Overlap with genomic annotations for six candidate causal SNPs for a co-localized eQTL-meQTL pair that shows strong evidence of mediation.** Insertion rs538810149 was the lead *cis*-eSNP for expression probe ILMN\_1758173 ( $P=10^{-24}$ ) which captures expression of KMEM99 (Panel A). This eQTL co-localized with a meQTL associated with methylations at 3 CpG sites: cg13464004, cg15432367, and cg13672106 (Panel A). We observed strong evidence of partial correlation (residual  $r = -0.35$ ;  $P=3 \times 10^{-10}$ ) and mediation (SEM  $P=7 \times 10^{-4}$ ; SME  $P=5 \times 10^{-8}$ ). This SNP is in strong LD with rs547853790 ( $r^2=0.93$ ), rs7219451 ( $r^2=0.93$ ), rs35026300 ( $r^2=0.93$ ), rs8082176 ( $r^2=0.92$ ), and rs11422105 ( $r^2=0.86$ ). Panel B shows overlap of candidate causal variants with transcription factor binding sites, DNase-I hypersensitivity sites, histone marks, and conservation among vertebrates, and GWAS SNPs (in that order). Panel B regions are color-coded to match the regions highlighted in Panel A. None of these SNPs show striking overlap with any of the regulatory features examined, other than rs11422105 which resides within a 10-tissue DNase-I hypersensitivity site.